ELSEVIER

Contents lists available at ScienceDirect

## International Journal of Refrigeration

journal homepage: www.elsevier.com/locate/ijrefrig



# Investigation of a refrigeration system based on combined supercritical CO<sub>2</sub> power and transcritical CO<sub>2</sub> refrigeration cycles by waste heat recovery of engine



Youcai Liang<sup>a,b</sup>, Zhili Sun<sup>c</sup>, Meirong Dong<sup>a</sup>, Jidong Lu<sup>a</sup>, Zhibin Yu<sup>b,\*</sup>

- <sup>a</sup> School of Electric Power, South China University of Technology, Guangzhou, Guangdong 510640, China
- <sup>b</sup> Systems, Power & Energy Research Division, School of Engineering, University of Glasgow, Glasgow G12 8QQ, UK
- <sup>c</sup> Tianjin Key Laboratory of Refrigeration Technology, Tianjin University of Commerce, China

### ARTICLE INFO

Article history: Received 9 September 2019 Revised 5 March 2020 Accepted 29 April 2020 Available online 16 May 2020

Keywords:
Refrigerated truck
Supercritical CO<sub>2</sub> power cycle
Transcritical CO<sub>2</sub> refrigeration cycle
Waste heat recovery

### ABSTRACT

The majority of the energy in the fuel burned in the internal combustion engines is lost in the form of waste heat. To address this issue, waste heat recovery technology has been proposed to increase the overall efficiency of engine. This paper investigates a heat driven cooling system based on a supercritical CO<sub>2</sub> (S-CO<sub>2</sub>) power cycle integrated with a transcritical CO<sub>2</sub> (T-CO<sub>2</sub>) refrigeration cycle, aiming to provide an alternative to the absorption cooling system. The combined system is proposed to produce cooling for food preservation on a refrigerated truck by waste heat recovery of engine. In this system, the S-CO<sub>2</sub> absorbs heat from the exhaust gas and the generated power in the expander is used to drive the compressors in both S-CO<sub>2</sub> power cycle and T-CO<sub>2</sub> refrigeration cycle. Unlike the bulky absorption cooling system, both power plant and vapour compression refrigerator can be scaled down to a few kilo Watts, opening the possibility for developing small-scale waste heat driven cooling system that can be widely applied for waste heat recovery from IC engines of truck, ship and train. A new layout sharing a common cooler is also studied. The results suggest that the concept of S-CO<sub>2</sub>/T-CO<sub>2</sub> combined cycle sharing a common cooler has comparable performance and it is thermodynamically feasible. The heat contained in exhaust gas is sufficient for the S-CO<sub>2</sub>/T-CO<sub>2</sub> combined system to provide enough cooling for refrigerated truck cabinet whose surface area is more than 105 m<sup>2</sup>.

© 2020 The Author(s). Published by Elsevier Ltd.

This is an open access article under the CC BY license. (http://creativecommons.org/licenses/by/4.0/)

# Étude d'un système frigorifique basé sur un cycle énergétique au CO<sub>2</sub> supercritique combiné à un cycle frigorifique au CO<sub>2</sub> transcritique par récupération de la chaleur résiduelle du moteur

Mots clés: Camion frigorifique; Cycle énergétique au CO2 transcritique; Cycle frigorifique au CO2 transcritique; Récupération de chaleur résiduelle

### 1. Introduction

Refrigerated truck is necessary for maintaining the quality and prolonging the shelf-life of fresh, frozen and perishable products during transportation. With respect to a typical diesel engine

\* Corresponding author: Tel.: +44 (0) 141 330 2530. E-mail address: Zhibin.Yu@glasgow.ac.uk (Z. Yu). aboard trucks, only less than 45% of the combustion energy can be converted to shaft power output, the residential energy is mostly lost by means of the exhaust gas and jacket water (Dolz et al. 2012). Hence, there is a demand of developing concepts for utilizing the waste heat to meet the cooling demand.

An ideal solution would be adopting a technology that can convert heat into cooling directly. Thermally powered cooling technologies have been investigated and some effort has been de-

### **Abbreviations** COP performance of coefficient CFC chlorofluorocarbon **HCFC** hydrochlorofluorocarbon ORC organic Rankine cycle T-CO<sub>2</sub> transcritical carbon dioxide cycle S-CO<sub>2</sub> supercritical carbon dioxide cycle VCC vapour compression cycle WHR waste heat recovery Symbols efficiency η specific entropy (kJ.kg<sup>-1</sup>) S h specific enthalpy (kJ.kg<sup>-1</sup>) mass flow rate (kg.s<sup>-1</sup>) m exergy (kW) E Т temperature (K) Q heat (kW) W work (kW) exergy destruction (kW) I safety factor ф K total heat transfer coefficient ( $W.m^{-2}.K^{-1}$ ); Α surface area (m<sup>-2</sup>) **Subscripts** compressor com expander exp recuperator rec cond condenser in inlet ambient air working fluid in S-CO2 cycle $f_1$ working fluid in T-CO2 cycle $f_2$ net power output net eva evaporator exhaust gas g

voted to the utilization of the vast amount of the waste energy of diesel engine (Shu et al., 2013). There are two conventional heat driven refrigeration systems, absorption refrigeration and adsorption refrigeration, which differs from vapour compression refrigeration system due to utilization of thermal energy source instead of electric energy. Absorption refrigeration can be considered as a refrigeration technology in terms of vaporization of liquid. The heat source transfers thermal energy to the strong solution and separates refrigerant and absorbent, while the refrigerant uptakes the heat from external environment during evaporation and makes the temperature lower. Among all the working fluids, ammonia -water (refrigerant-absorbent) and water-lithium bromide (refrigerant- absorbent) are the most popular ones in application. Lithium bromide-water systems are fairly well developed and have already been in use for many years but water-ammonia systems are used in the fields where the refrigeration temperature is above 0  $^{\circ}\text{C}$  since its refrigerant is water. NH $_3\text{-H}_2\text{O}$  absorption refrigeration system have shown the feasibility in trawler chiller fishing vessels (Fernández -Seara et al. 1998). Manzela (2010) introduced an absorption refrigeration system driven by engine exhaust gas. Liang et al. (2013, 2014, 2018) conducted several investigations of waste heat recovery (WHR) of marine engine by integrating absorption refrigeration cycle with steam Rankine cycle. From the literature review it can be learned that the exhaust heat of engine can be used as a suitable heat source for the absorption refrigeration cycle. However, the absorption chillers generally used for large-scale

industrial applications and large scale marine engines. Waste heat recovery from small sources such as automobile engines is scarce. Furthermore, the coefficient of performance (COP) is generally low for single-stage absorption cycle systems at a relatively small scale.

Adsorption refrigeration is also a heat driven refrigeration technology. As explained by Ruthven (1984), adsorption occurs at the surface interface of two phases, heating-desorption-condensation phase in which the adsorbate was desorpted from the absorbent then the condensed liquid adsorbate was transferred into the evaporator, and cooling-adsorption-evaporation phase in which the liquid adsorbate evaporates and makes cooling effect. Wang et al. (2006) conducted a comprehensive review on the adsorption refrigeration and it is proposed to be used in waste heat recovery for both icemakers and air conditioners. Wang's research group (Gao et al. 2016, Zhu et al. 2016, Gao et al. 2019) were devoted to a series of research on solid sorption freezing cycle for refrigerated trucks.

In general, both absorption and adsorption cooling systems have their own characteristics and advantage, and both can be powered by waste heat energy. Compared with an absorption system, the adsorption cooling system has the advantages of mechanical simplicity, high reliability (Liu and Leong, 2005) and downsizing (Tiwari and Parishwad 2012), while it needs to more than two adsorption beds for continuous refrigeration process. Furthermore, the pressure loss of the vapor in the adsorption refrigeration system is much higher than that of the absorption refrigeration system. In general, the COP of both is much lower than that of the mechanical compression refrigeration system. The work on COP improvement becomes the priority for the further development and application of both absorption and adsorption refrigeration systems in future.

Ejector refrigeration is another heat driven refrigeration technology with simple structure, high system reliability. The steam ejector refrigeration chiller has been widely used in air conditioner. The use of refrigerants with low boiling point has great potential in application of refrigerated trucks for its downsizing and lightweight. However, the ejector refrigeration system has not been widely used in the refrigerated as expected. The main reason is that it is difficult to meet the refrigeration requirements of refrigeration transportation under high condensation temperature. Due to the limitation of cold source available in transportation equipment, ambient air is usually used as cold source, and the heat transfer coefficient is small. In the hot climate areas, the condensation temperature and pressure of the system are higher. However, it is necessary to maintain the temperature between - 18  $^{\circ}$ C to +13  $^{\circ}$ C for different foods in the process of cold chain logistics transportation (International Institute of Refrigeration 1995). As a result, the evaporation pressure requires to be lower. For the performance of ejector is closely related to the injection coefficient. Increasing the pressure ratio will significantly reduce the performance of the ejector. The decrease of the refrigeration temperature will result in a sharp reduction in the efficiency of the injection system. When the ratio of ejector back pressure to ejector pressure exceeds a certain value, the ejector coefficient will drop sharply. This means that under a high condensing temperature, the corresponding condensing pressure is also high, and it is difficult for the traditional ejector to achieve a lower refrigeration temperature. Therefore, the conventional heat driven ejector refrigeration is not feasible to be used on refrigerated truck.

Mechanical vapour compression refrigeration systems have been widely employed in most refrigerated trucks at present. The compressors are normally driven by the mechanical power from engines, which certainly increase the fuel consumption and greenhouse gas emissions. If the mechanical power required can be met by waste heat recovery of engine, the fuel consumption would be reduced. For this reason, the concept of combining organic Rankine cycle (ORC) and vapour compression cycle (VCC) was proposed as an alternative refrigeration method by Prigmore and Barber (1975). Compared to the thermally powered absorption cooling technologies, the ORC-VCC has some potential advantages in terms of performance and simplicity. Furthermore, the VCC powered by an ORC can make use of the heat source throughout the year (Wang et al., 2011a) to provide either cooling or electricity when cooling is not required (Wang et al., 2011b), increasing the operational flexibility and improving the economic profitability. Although the ORC-VCC is attractive providing cooling by waste heat recovery, there are still some problems for its practical applications, including the decomposition issue of the organic working fluid in ORC and the difficulty in finding suitable environmentally friendly refrigerants in VCC (Liang et al., 2018).

With respect to most diesel engines, the maximum temperature of the exhaust gas approximately ranges from 720 to 870 K (Zheng et al., 2019), while the decomposition temperature of most working fluids is below 600 K. By considering the decomposition issue of organic working fluids, ORC application is limited in the field of engine WHR. Furthermore, the size and weight of the expander need to be considered for the economic factor. That is the reason why ORC has not been applied in automobile engine WHR yet although it has been investigated and tested for a long time. The supercritical carbon dioxide Brayton cycle was proposed by Fether (1968) and Angelino (1968) because carbon dioxide is a nature refrigerant, which is environmentally friendly, lowcost, non-toxic, non-flammable, non-corrosive and has good chemical stability. When comparing the operational principles of supercritical Brayton cycle (SBC) and ORC or steam Rankine technology, the main difference is that in a SBC the working fluid remains at supercritical condition through the whole cycle and the fluid is compressed with a compressor instead of a pump. The high fluid density of S-CO<sub>2</sub> enables extremely compact turbomachinery designs, which is significantly attractive for the practical applications of waste heat recovery aboard vehicles. As the heat exchangers and turbines become more and more efficient, CO2-based power cycles, including both supercritical and transcritical cycle, attract more and more attention in recent years since they are more suitable for high temperature WHR.

In Combs's (1977) investigation, the performance of a supercritical CO2 engine was studied for propulsion power in a naval ship application using basic thermodynamics approach. It is reported that the supercritical CO<sub>2</sub> cycle can achieve higher power and efficiency with significant fuel saving. Recently, Sarkar (2015) and Ahn et al. (2015) reviewed the literature related to the current research and development of supercritical CO<sub>2</sub> cycles. It is recognized that nuclear, fossil fuel, waste heat and other high temperature heat source are the potential application areas of S-CO<sub>2</sub>. A comprehensive comparison of different S-CO<sub>2</sub> Brayton layouts was conducted by Wang (2017), in which S-CO<sub>2</sub> Brayton cycle is considered to be integrated with the molten salt solar power tower systems. A supercritical carbon dioxide (SC-CO<sub>2</sub>) based regenerative recompression Brayton cycle (RRCBC) was proposed for shipboard applications in terms of waste-heat-recovery-system (WHRS) by Sharma (2017). Echogen Power Systems (EPS) company (Persichilli et al., 2012; Persichilli et al., 2011) carried out preliminary tests of 250 kW CO<sub>2</sub> heat engine by recovering exhaust gas waste heat, which indicates the possibility of recovering the waste heat of engine exhaust gas. It is also reported that the Levelized Cost of Electricity (LCOE) is calculated at an average USD \$0.025 per kWh for the CO<sub>2</sub>-based heat engine. These studies proved the great potential of S-CO<sub>2</sub> in the field of waste heat recovery of engine. In the S-CO<sub>2</sub> cycle, recuperator is typically used to further utilize the energy at turbine outlet to increase cycle efficiency. However, the total heat load of the hot S-CO2 cannot be recovered entirely by the recuperator due to the limited heat exchanger effectiveness. Therefore, Song et al. (2018) and Liang et al. (2019) proposed to integrate S- $CO_2$  with an ORC, which is used as a bottoming cycle for the further recover the residual heat load.

The concept of CO<sub>2</sub> vapor compression refrigeration system was first proposed by Alexander Catlin Twining in 1850, but CO2 was first used actually in a vapor compression system to produce ice by Thaddeus Lowe in 1866 (Ma et al., 2013). However, due to poor technology at that time, the CO2 refrigeration presents a low refrigeration efficiency and its application was not popular. Interest in CO<sub>2</sub>-based refrigeration system was renewed in the early 1990s due to the phase-out of ozone depleting refrigerants. In 1987, Montreal Protocol and its amendments (Protocol, 1987) gave a deadline to the use of chlorofluorocarbon (CFC) and hydrochlorofluorocarbon (HCFC) refrigerants, which are being phased out. As a result, natural refrigerants, such as carbon dioxide, ammonia and hydrocarbons, have been found to be attractive refrigerants in refrigeration system. Amongst the natural refrigerants, carbon dioxide seems to be the most promising one, especially as the natural refrigerant for automotive air conditioning systems. Other factors like safety requirements, extra tax on HFC systems and limitations on the maximum amount of HFC charge that can be used on a single system also attribute to  ${\rm CO}_2$  acceptability in commercial refrigeration. For refrigeration purpose, subcritical CO2 or transcritical CO<sub>2</sub> (T-CO<sub>2</sub>) refrigeration would be chosen based on the heat sink temperature. One of the first T-CO<sub>2</sub> systems was a prototype automotive air conditioning system built and tested by Lorentzen and Pettersen (1993), and further reported by Pettersen (1994). The result indicated that transcritical CO2 based automotive air conditioning has comparable performance with that of a R12 system, which encouraged further development of transcritical CO<sub>2</sub> system. The technical feasibility of using transcritical CO<sub>2</sub> refrigeration cycle for engine waste heat recovery has been verified and guaranteed as it has already been used in vehicle air conditioning devices (Kim et al., 2009; Tao et al., 2010).

From the literature review above, there is a possibility to integrate a S-CO2 power cycle with a CO2 based refrigeration cycle, which will adopt the similar concept of ORC-VCC consisting a power cycle and refrigeration cycle. However, due to its high operation pressure, the design of expander and compressor is the main concern for the practical application. Daikin industries Ltd (Ohkawa et al., 2002) developed a swing type compressor with high efficiency and reliability for CO2 heat pump water heaters. Reducing the ratio of cylinder height to cylinder diameter was introduced to minimize the leakage loss during operation. To reduce the stress intensity and the leakage caused by the high operation pressure of CO<sub>2</sub>, Dreiman et al. (2004) designed two cylinder rotary hermetic compressors. The test results showed that volumetric efficiency ranged between 0.4 and 0.8 and the compressor efficiency was up to 0.6. In Chinen's study (2014), the COP of a CO2 rotary compressor was enhanced by optimizing the design of the discharge pathway from the compression chamber, including the discharge-port diameter, and adjusting the flux level of the motor. Stosic et al. (2002, 2006) proposed that for the twin screw machines, a major problem is that the pressure difference between entry and exit creates very large radial and axial forces on the rotors whose magnitude and direction is independent of the direction of rotation. He developed a combined compressor expander, in which rotor forces created by the compression and expansion processes can be partially balanced in order to eliminate the axial forces and reduce the radial bearing forces. The development of different type compressors promoted the investigation and development of the CO<sub>2</sub> based thermodynamic

In this paper, an integrated system of S-CO<sub>2</sub> and T-CO<sub>2</sub> is proposed to provide refrigeration by waste heat recovery of refrigerated truck engine. In spite of numerous studies on individual S-

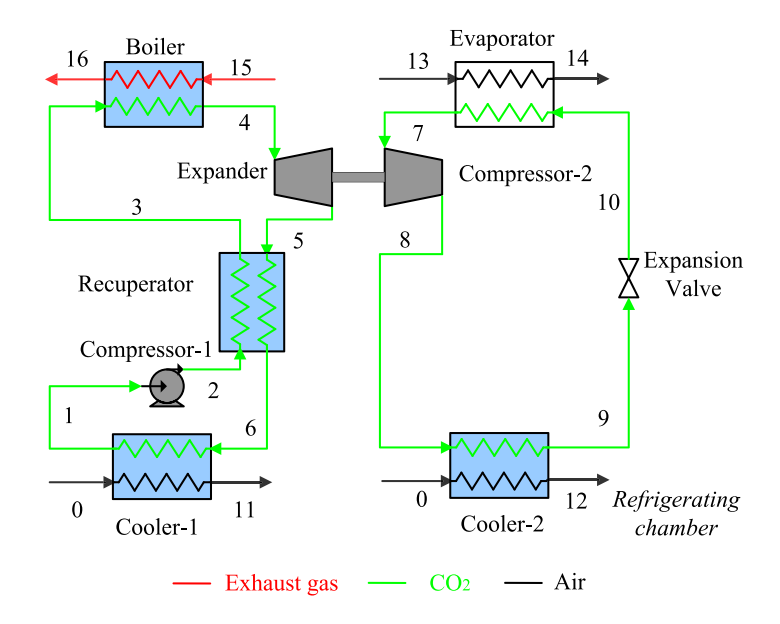


Fig. 1. Schematic diagram of the S-CO<sub>2</sub>/T-CO<sub>2</sub> combined cycle with two separate coolers.

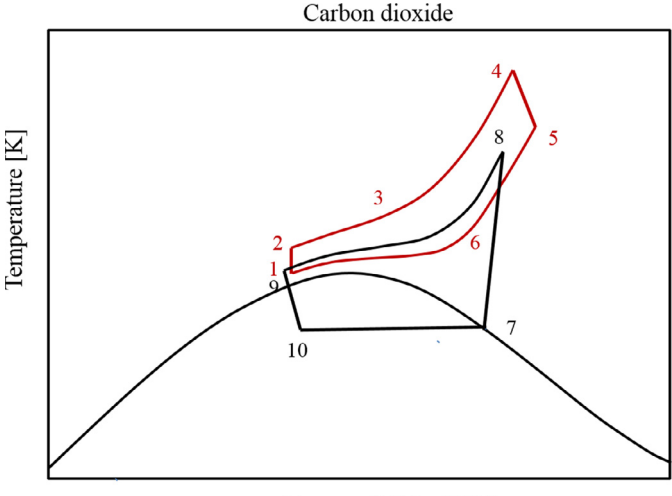
CO<sub>2</sub> power cycle or T-CO<sub>2</sub> refrigeration cycle, no research mentioned the concept of integrating S-CO<sub>2</sub> with T-CO<sub>2</sub> for cooling purpose, especially by waste heat recovery of engine. In order to make the proposed system more compact, the layout sharing a common cooler is also studied. A comprehensive energy and exergy analysis evaluation was carried out to demonstrate the potential of the proposed S-CO<sub>2</sub>/T-CO<sub>2</sub> refrigeration system on refrigerated trucks.

### 2. System description

A refrigerated truck with an engine rated power of 243 kW is analyzed. The air fuel ratio in this study is set to be 19.7 under the rated condition. Under the hypothesis of perfect combustion of diesel fuel, the composition of the exhaust gas was calculated by mass:  $CO_2 = 15.1\%$ ,  $H_2O = 5.5\%$ ,  $N_2 = 71.6\%$ ,  $O_2 = 7.8\%$ . This composition is used to evaluate the thermodynamic properties of the heat source.

Fig. 1 represents the schematic diagram of the proposed S-CO<sub>2</sub>/T-CO<sub>2</sub> combined cycle with two separate coolers. The exhaust gas of the engine is used to drive the proposed combined cycle, which consists of a supercritical CO2 power cycle and a transcritical CO<sub>2</sub> refrigeration cycle. In this system, the power cycle absorbs heat from the exhaust gas and the generated power in the expander is used to drive the compressors in both power cycle and that in the refrigeration cycle. Since the temperature of CO<sub>2</sub> stream exiting the expander outlet remains high, a recuperator is adopted to further utilize the energy to improve the thermal efficiency of power cycle. As this system will be used aboard a refrigerated truck, both coolers are air-cooled type for the limitation of its application environment. Such a refrigeration system aims to provide sufficient cooling for the refrigerated truck cabinet to preserve food or other goods during transporting. The Temperaturespecific entropy (T-S) diagram of the combined cycle is shown in Fig. 2.

Liang et al. (2019) mentioned that the isobaric specific heat capacity of carbon dioxide changes dramatically near the pseudocritical point (the temperature at which the specific heat reaches a peak for a given pressure) and decreases gradually away from the pseudo-critical point. This phenomenon can provide explanations for the dramatic changes results pseudo-critical point in the following.



Entropy [kJ. kg<sup>-1</sup>.K<sup>-1</sup>]

Fig. 2. Temperature-specific entropy diagram of the  $S-CO_2/T-CO_2$  combined cycle.

### 3. Assumptions and Modeling

A program developed based on MATLAB and the REFPROP database is adopted to study the thermodynamic performance of the system. The following assumptions are applied for modeling:

- (1) The ambient temperature remains constant of 25 °C (Sun et al., 2019) since it is usually taken as the reference temperature.
- (2) The whole system are operated under a steady state.
- (3) Heat loss and pressure loss are neglected in all pipes and components.
- (4) The temperature of the exhaust gas is higher than the acid dew point after heat transfer, and the acid dew point is assumed to be 120 °C to avoid the corrosion of the pipe and heat exchanger.
- (5) The pinch point in the boiler is 30 °C and that in the other heat exchangers is 5 °C to ensure the feasible design of economical heat exchanger.

 Table 1

 Required refrigerating capacity under different refrigeration temperatures.

Required refrigeration capacity [W]
3685.86
4423.02
5160.2
5897.36
6634.54

- (6) The isentropic efficiency of the expander and compressors is 0.8 and 0.9 respectively, and the efficiency of the recuperator is 0.9.
- (7) Based on the heat source temperature and the heat sink temperature (ambient air), the maximum temperature, the minimum temperature and minimum pressure in the S-CO<sub>2</sub> power cycle are assumed to be 380 °C, 32 °C and 7500 kPa respectively.

The required cooling capacity of the refrigerated truck is given by (Gao et al., 2016)

$$Q_{cabinet} = \varphi \cdot K_{cabinet} \cdot A_{cabinet} \cdot (T_0 - T_{cabinet,in})$$
 (1)

 $\phi$  – safety factor, the minimum value is 1.75 and it is set to be 2 in this study.

 $K_{cabinet}$  - total heat transfer coefficient, 0.7 W. (m²•K)-1, the ATP classifies insulated vehicles and bodies as either Normally Insulated Equipment (K equal or less than 0.7 W/(m²K)) or Heavily Insulated Equipment (K coefficient equal or less than 0.4 W/(m²K) (Tassou et al., 2012), the truck studie in this paper is taken as Normally Insulated Equipment;

 $A_{cabinet}$  - surface area of the cabin, m<sup>2</sup>;

 $T_0$  - ambient temperature, which is set to be 25 °C;

 $T_{target}$  – target refrigeration temperature in cabin, °C.

The size of the cabinet (the storage bin for goods) is  $9400 \times 2450 \times 2500$  mm, whose surface area is 105.31 m². Based on Eq. (1), the required cooling capacities under different target refrigeration temperatures are shown in Table 1. It can be noted that the required cooling capacity is higher when the refrigeration temperature is lower for a higher temperature difference between the cabinet and ambient air. The maximum refrigeration capacity of 6634.54 W is required when the target refrigeration temperature is -20 °C.

The exergy at state point i in the system can be defined as:

$$E_i = m_f[(h_i - h_0) - T_0(s_i - s_0)]$$
(2)

Expressions for exergy destruction rate and exergy efficiency is shown in table 2.

$$Ex_{ph} = (h - h_0) - T_0(s - s_0)$$

The net power output of S-CO<sub>2</sub>:

$$W_{net} = W_{exp} - W_{com-1} \tag{3}$$

The thermal efficiency of S-CO<sub>2</sub>:

$$\eta_{S-CO2} = \frac{W_{net}}{Q_{boiler}} \tag{4}$$

The cooling coefficient of performance:

$$COP_c = \frac{Q_{eva}}{W_{com-2}} = \frac{Q_{eva}}{W_{net}} \tag{5}$$

The exergy destruction in S-CO<sub>2</sub> power cycle:

$$I_{S-CO2} = I_{com-1} + I_{exp} + I_{boiler} + I_{rec} + I_{cooler-1}$$

$$\tag{6}$$

The exergy destruction in T-CO<sub>2</sub> refrigeration cycle:

$$I_{T-CO2} = I_{com-2} + I_{valve} + I_{eva} + I_{cooler-2}$$
 (7)

The total exergy destruction caused in this system:

$$I_{total} = I_{S-CO2} + I_{T-CO2} \tag{8}$$

In this system, the two compressors are driven by the power generated by the expander in S-CO<sub>2</sub>, which can be taken as the energy consumption within the system. Therefore, the net energy input is the exhaust gas released in the boiler and the energy output is the useful cooling produced in the evaporator. The exergy efficiency of the combined cycle can be defined as useful exergy output to the exergy input:

$$\eta_{II} = \frac{Q_{eva}(T_0/T_{t \text{ arg }et} - 1)}{(E_{15} - E_{16}) + W_{com-1}}$$
(9)

### 4. Model validation

Since there is no published literature about the proposed combined cycle that consists a supercritical CO<sub>2</sub> power cycle and a transcritical CO<sub>2</sub> refrigeration cycle, the established S-CO<sub>2</sub> power cycle and T-CO<sub>2</sub> refrigeration cycle need to be validated independently. The model of the supercritical CO<sub>2</sub> power cycle with recuperator has been validated in our previous research [24] and it shows that the error between the paper and the reference (Manente and Lazzaretto, 2014) is 2.25%. For the transcritical CO<sub>2</sub> refrigeration cycle, two operation conditions are compared. When T<sub>9</sub> is 40 °C, the error of COP is only 0.1% and it is 2.36% When T<sub>9</sub> is 35 °C.

### 5. Results and discussion

The performance of the combined cycle is affected by many factors. A detailed analysis for different operation conditions has been carried out.

5.1. The S-CO<sub>2</sub>/T-CO<sub>2</sub> combined cycle with two separated coolers

In this part, two separate coolers are used in S-CO<sub>2</sub> power and T-CO<sub>2</sub> refrigeration cycles, as shown in Fig. 1. The low-side pressure of the S-CO<sub>2</sub>, the expander inlet temperature and the outlet temperature are set to be 7500 kPa and 380 °C and 305 °C respectively. In this system, the operation pressure of S-CO<sub>2</sub> power cycle influences the operation of the T-CO<sub>2</sub> refrigeration cycle since the power consumed by the compressor-2 in T-CO<sub>2</sub> is provided by the expander in S-CO<sub>2</sub>. Therefore, the effect of the high-side pressure (the expander inlet pressure) in S-CO<sub>2</sub> power cycle is analyzed and discussed in this part.

Fig. 3 shows the effect of expander inlet pressure on the expander power output, compressor power input and the net power output of the S-CO<sub>2</sub> power cycle. It can be observed that the curves show an increasing trend as the expander inlet pressure increases. It is known that the enthalpy difference across the expander increases as the inlet pressure (for a given outlet pressure of 7500 kPa), thus the power output of the expander increases. Meanwhile, a higher compressor power input will be required for a higher pressure difference across the compressor. By subtracting compressor input from the expander power output, the net power output of the S-CO<sub>2</sub> power cycle is still increasing though the curve becomes smoother.

It has to be mentioned that the condensation temperature of T-CO<sub>2</sub> refrigeration cycle is fixed to be 305 K. In this combined cycle, the pressure drop across the expander is proportional to the pressure difference across the compressor. Subsequently, the discharged pressure of compressor in T-CO<sub>2</sub> cycle increases with the expander inlet pressure. As a result, the discharged temperature of the compressor is raised, as shown in Fig. 4. The curves also indicate that a higher discharge temperature of the compressor-2 will be obtained when the evaporation pressure becomes lower. As the

**Table 2**Expressions for energy balance, exergy destruction and exergy efficiency of components.

Components	Energy balance	Exergy destruction	Exergy efficiency [Sun et al., 2019]
Compressor-1	$W_{com-1} = m_{f1}(h_2 - h_1)\eta_{is,com-1} = \frac{h_{2s} - h_1}{h_2 - h_1}$	$I_{com-1} = W_{com-1} + E_1 - E_2$	$\eta_{ex,com-1} = \frac{E_2 - E_1}{W_{com-1}}$
Expander	$W_{exp} = m_{f1}(h_4 - h_5)\eta_{is,exp} = \frac{h_4 - h_5}{h_4 - h_{5s}}$	$I_{exp} = E_4 - E_5 - W_{exp}$	$\eta_{ex,exp} = rac{W_{exp}}{E_4 - E_5}$
Boiler	$Q_{boiler} = m_{f1}(h_4 - h_3)Q_{boiler} = m_g(h_{15} - h_{16})$	$I_{boiler} = E_3 + E_{15} - E_4 - E_{16}$	$\eta_{ex,boiler} = \frac{E_4 - E_3}{E_{15} - E_{16}}$
Recuperator	$Q_{rec} = m_{f1}(h_3 - h_2)h_5 - h_6 = h_3 - h_2$	$I_{rec} = E_2 + E_5 - E_3 - E_6$	$\eta_{ex,rec}=rac{E_5-E_6}{E_3-E_2}$
Cooler-1	$Q_{cooler-1} = m_{f1}(h_6 - h_1)$	$I_{cooler-1} = E_0 + E_6 - E_1 - E_{11}$	$\eta_{ex,cooler-1} = rac{E_{11}-E_0}{E_6-E_1}$
Expansion valve	$h_9 = h_{10}$	$I_{valve} = E_9 - E_{10}$	$ \eta_{ex,valve} = \frac{E_{10}}{E_9} $
Compressor-2	$W_{com-2} = m_{f2}(h_8 - h_7)W_{com-2} = W_{exp}\eta_{is,com-2} = \frac{h_{8s} - h_7}{h_8 - h_7}$	$I_{com-2} = W_{com-2} + E_7 - E_8$	$ \eta_{ex,com-2} = \frac{E_8 - E_7}{W_{com-2}} $
Evaporator	$Q_{eva} = m_{f2}(h_7 - h_{10})$	$I_{eva} = E_7 - E_{10} + Q_{eva} (1 - \frac{T_0}{T_{t  arget}})$	$\eta_{ex,eva} = rac{(rac{T_0}{T_{ m rarget}}-1)Q_{eva}}{E_{10}-E_7}$
Cooler-2	$Q_{cooler-2} = m_{f2}(h_8 - h_9)$	$I_{cooler-2} = E_0 + E_8 - E_9 - E_{12}$	$\eta_{ex,cooler-2} = \frac{(1 - \frac{T_0}{T_{12}})Q_{cooler-2}}{E_8 - E_9}$

**Table 3**Comparison of the present calculated results with the published literature for T-CO<sub>2</sub>.

Parameter	Reference (Baheta et al., 2015)	Calculated	Error	Reference (Baheta et al., 2015)	Calculated	Error
P7 (Mpa)	4	-	4	-		
P8 (Mpa)	10	-	10	-		
T9 (°C)	40	-	35	-		
ηis,com-2	100%	-	100%	-		
COP	3.24	3.2431	0.10%	3.82	3.91	2.36%

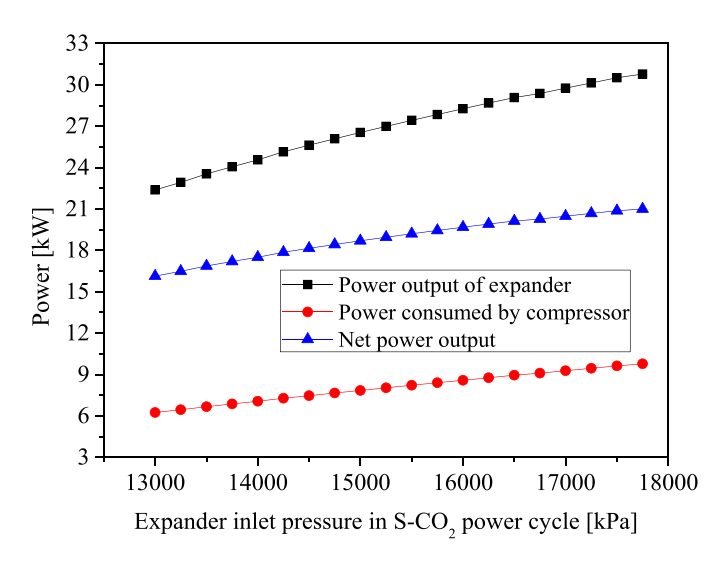


**Fig. 3.** Power output of the expander, power consumed by compressor-1 and the net power output change with the expander inlet pressure in when the evaporation temperature in refrigeration cycle is -5 °C.

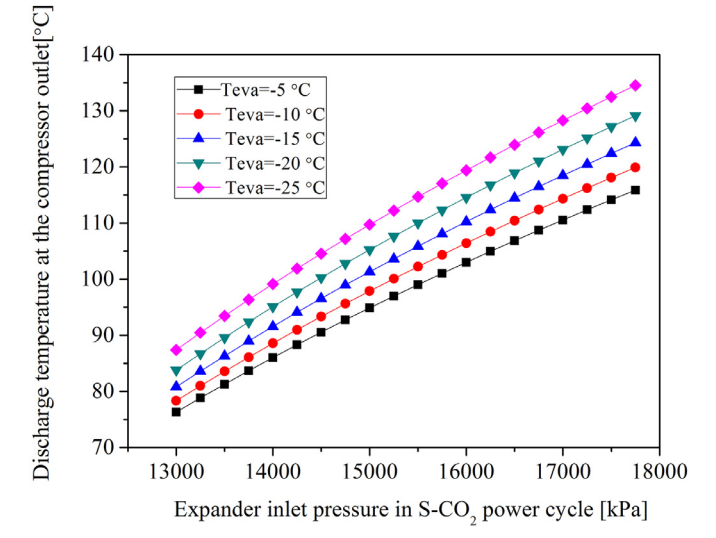


Fig. 4. Discharge temperature of the compressor in T-CO<sub>2</sub> refrigeration cycle.

evaporation temperature becomes lower, a lower suction pressure would require more power to obtain a higher compression ratio across the compressor, resulting in a higher compressor discharge temperature. This is the main reason why the compressor is often ruined when it continues running at low ambient temperatures.

Fig. 5 represents the variation of the cooling capacity changing with the expander inlet pressure. The cooling output is the most important evaluation parameter since it is the sole useful output in the proposed combined cycle. As shown in Fig. 5, the cooling capacity increases first and then decreases as the expander inlet pressure increases. The peaks appear at different expander inlet pressures for different evaporation temperatures. When the evaporation temperature is higher than -15 °C, the variation of the cooling capacity becomes smother. When the evaporation temperature is -20 °C or lower, the cooling capacity increases dramatically when the expander inlet pressure increases from 13000 kPa

to 13500 kPa. This is because the pseudo-critical points appear at different temperatures under different pressures, as mentioned above. The specific heat capacity increases first and then decreases as the temperature increases, there is a peak specific heat capacity at the pseudo-critical point. That is why there is a rapid growth for the cooling capacity when the expander inlet pressure varies from 13000 kPa to 13500 kPa. The maximum value of the cooling capacity is more than 49 kW for  $T_{eva}$ =-25 °C, which increases to more than 72 kW for  $T_{eva}$ =-5 °C. Therefore, such a system can provide sufficient cooling for a refrigerated truck with a cabinet over 105 m², whose required cooling capacity is only 3.317 kW, as shown in table 1.

The calculated *COP* of cooling is the ratio of cooling capacity to the compressor power (net power output in S-CO<sub>2</sub>), which strongly depends on the operating conditions, especially absolute temperature and temperature difference between heat sink and the target refrigeration temperature. In Fig. 6, when the evaporation tem-

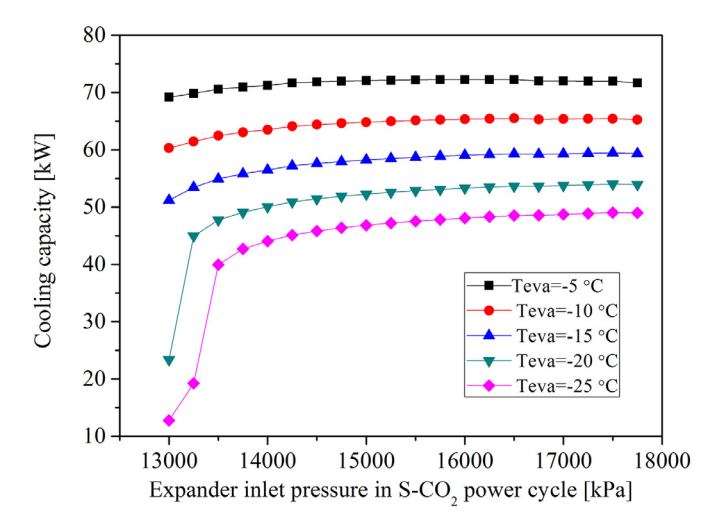


**Fig. 5.** Effect of the expander inlet pressure on the cooling capacity in  $T\text{-}CO_2$  refrigeration cycle.

perature  $T_{eva}$ =-5 °C and  $T_{eva}$  =-10 °C, the cooling COP decreases with the expander inlet pressure. When the evaporation temperature decreases below -15 °C (included), there is an optimum COP value as the expander inlet pressure increases. The variation of the net power output in Fig. 4 and the variation of cooling capacity in Fig. 6 determine the variation of COP shown in Fig. 6.

Fig. 7 shows the exergy efficiency of all the components when the pressure at the expander inlet is 13000 kPa. It can be learned that the expansion valve in T-CO<sub>2</sub> presents the maximum value among all the components, following by two compressors, expander, and exergy efficiency of all heat exchangers is relatively low due to the temperature difference between the hot stream and cold stream.

To further assess the performance of the system, Grassmann diagram was used to show the exergy flow in terms of exergy and exergy destruction (Hinderink et al.,1999). Fig. 8 is the Grassmann diagram of the combined system when the expander inlet pressure is 13000 kPa in the power cycle. In the power cycle, it can be seen that the exergy input of the exhaust gas through the boiler is 43.73 kW, including 38.53 kW to the CO2 stream and 5.2 kW exergy destruction during heat transfer. And then 22.38 kW mechanical power is generated in the expander and 2.8 kW exergy destroyed during the expansion process. In the recuperator, exergy destruction can be up to 14.09 kW due to the large temperature

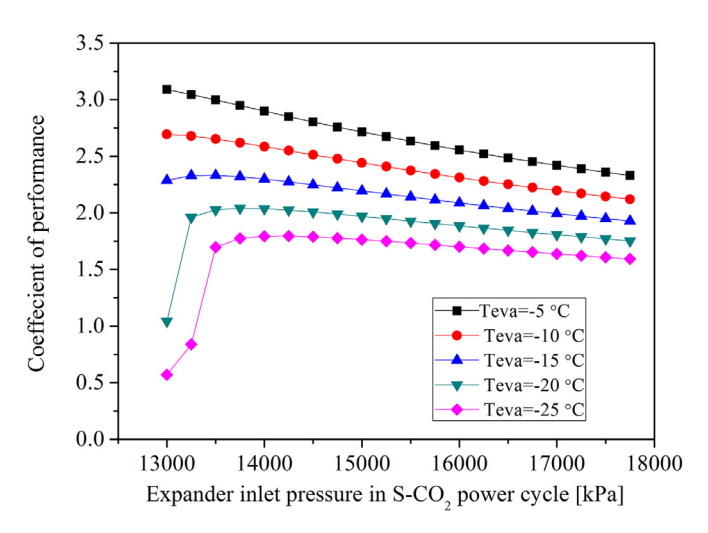


Fig. 6. Effect of the expander inlet pressure on the cooling COP in  $T\text{-}CO_2$  refrigeration cycle.

difference between the hot and cold stream. In the cooler-1, the exergy of working fluid deceases by 4.95 kW, including 3.39 kW exergy destruction and 1.56 kW exergy loss through ambient air. The pump consumes 6.25 kW to enhance the pressure, in which 5.69 kW transits to the working fluid and the other is destroyed in terms of exergy destruction. Therefore, the total exergy input of 49.98 kW (43.73+6.25), equals to the sum of exergy destruction in boiler (5.2 kW), exergy destruction in the expander (2.80 kW), exergy destruction in the recuperator (14.09 kW), exergy destruction and exergy loss in cooler-1 (1.87 kW and 3.08 kW respectively) and the exergy destruction in compressor-1 (0.56 kW).In the refrigeration cycle, the exergy input is provided by the power cycle and the amount is 22.38 kW. The total exergy destruction and loss in the refrigeration cycle is 16.05 kW. In that case, the final transiting cooling exergy is 6.33 kW.

The variation of exergy efficiency with expander inlet pressure for various evaporator temperatures is shown in Fig. 9. In this system, the power produced in S-CO<sub>2</sub> cycle is consumed by compressor-1 and compressor-2, rather than supplying mechanical power as output. According to Eq. (9), the output and input exergy of the proposed system is cooling provided by evaporator and the heat energy transferred in boiler respectively. For the same evaporation temperature, the variation trend of exergy efficiency in Fig. 9 is similar to that of the cooling capacity in Fig. 6. This is

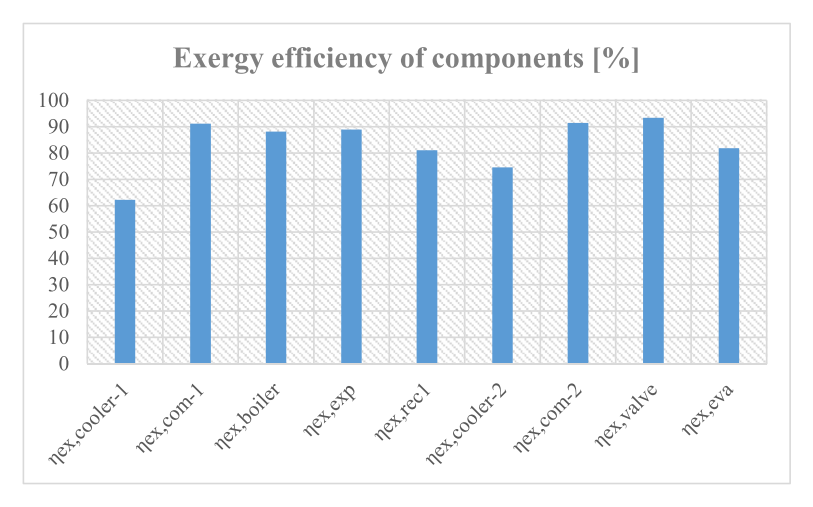


Fig. 7. Exergy efficiency of components when the pressure at the expander inlet is 13000 kPa.

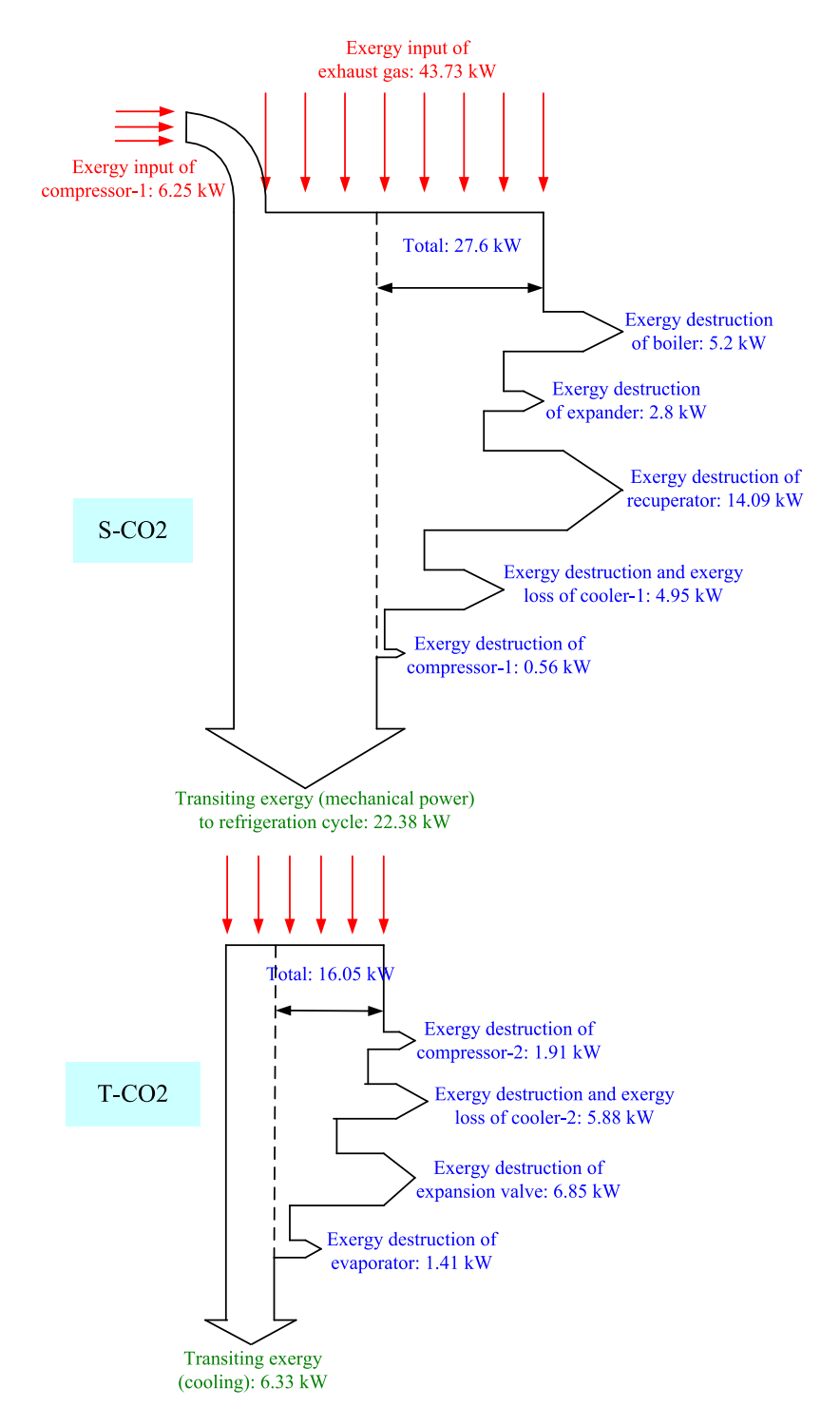


Fig. 8. Grassmann diagram of the proposed combined cycle when the inlet pressure at the expander inlet is 13000 kPa.

because the exergy output of cooling presents a similar variation with cooling capacity. However, the maximum exergy efficiency is achieved by the conditions  $T_{eva}$ =-25 °C for its higher cooling exergy output.

## 5.2. The $S-CO_2/T-CO_2$ combined cycle sharing a common cooler

Since both sub-cycles are using carbon dioxide as the working fluid, there is a possibility to share a common cooler to make the freezing system more compact and reduce the size and weight.

Different from the previous layout, the stream exiting recuperator (state 6) in  $S-CO_2$  and that exiting the compressor (8) in  $T-CO_2$  cycle both flow into the common cooler and are cooled down by the ambient air. In that case, the exiting temperature of  $S-CO_2$  is the same as that of  $T-CO_2$  (as shown in Fig. 8) and the state point 1 and point 9 are coincident. The temperature-entropy diagram of the proposed  $S-CO_2/T-CO_2$  combined cycle is shown in the Fig. 9.

The same concept was proposed and studied by Aphornratana et al. (2010), Saleh et al. (2016) and Li et al. (2013). Different from our investigation, the working fluids considered in these reference

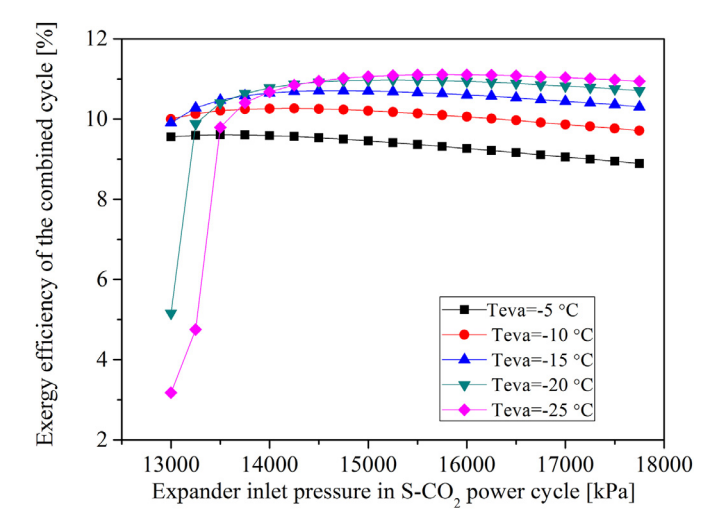


Fig. 9. The overall exergy efficiency of the combined cycle.

are organic working fluids, which cannot be used for high temperature waste heat recovery due to the decomposition issue. Furthermore, the proposed S-CO<sub>2</sub>/T-CO<sub>2</sub> combined cycle has greater potential in both size and weight for the turbomachinery, which is more attractive in waste heat recovery of vehicle.

### 5.2.1. Fixed maximum pressure in power cycle

Since the power cycle and the refrigeration share a common cooler, the pressure in cooler has great impact on the performance of both the supercritical  $\rm CO_2$  power cycle and the transcritical  $\rm CO_2$  refrigeration cycle. Therefore, the effect of the pressure in cooler is studied in this part. The maximum pressure in the power cycle is fixed to be 14000 kPa.

In the S-CO<sub>2</sub>/T-CO<sub>2</sub> combined cycle, the compressor-2 in refrigeration cycle is driven by the expander in the power cycle. For a fixed expander inlet pressure, the increase in the pressure in cooler leads to a lower pressure drop across the expander. In that case, the pressure difference across the compressor-2 also decreases, which results in a higher evaporation pressure and evaporation.

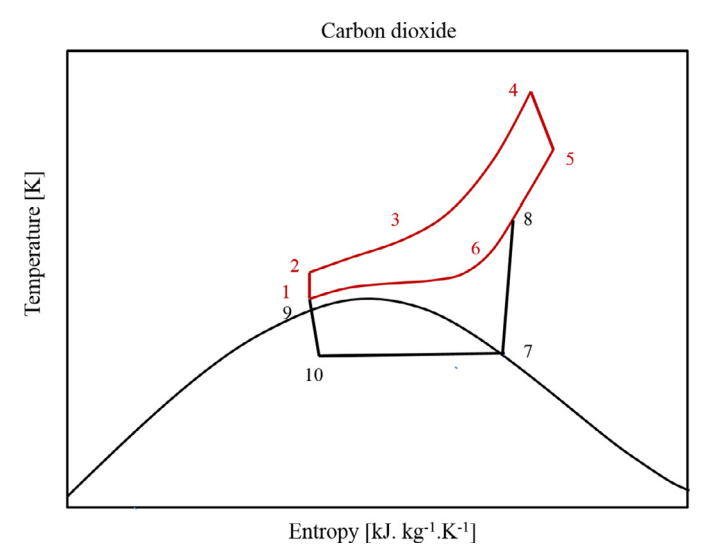


Fig. 11. Temperature-Enthalpy of the  $S-CO_2/T-CO_2$  combined cycle sharing a common cooler.

oration temperature in T-CO $_2$  cycle, as shown in Fig . 12. Furthermore, it can be noted that the cooling capacity also increases with the increasing pressure in cooler. Although the power generated in the expander decreases slightly, the mass flow rate of CO $_2$  in the refrigeration cycle increases for a lower pressure difference in the compressor-2. That is the reason why the cooling capacity keeps increasing as the pressure in the cooler increases.

Fig. 13 shows the contribution of each component on the exergy destruction under different pressures in the cooler. It is evident that for the operating conditions considered, the recuperator in S-CO<sub>2</sub> cycle contributes the most significant part of the total exergy destruction in the system. This result is attributable to the significant irreversibilities associated with heat transfer across the large temperature differences in the recuperator. In T-CO<sub>2</sub> cycle, the irreversibility across expansion valve is the maximum. This suggests that in order to improve the performance of the proposed system, special attention should be directed to reducing the irre-

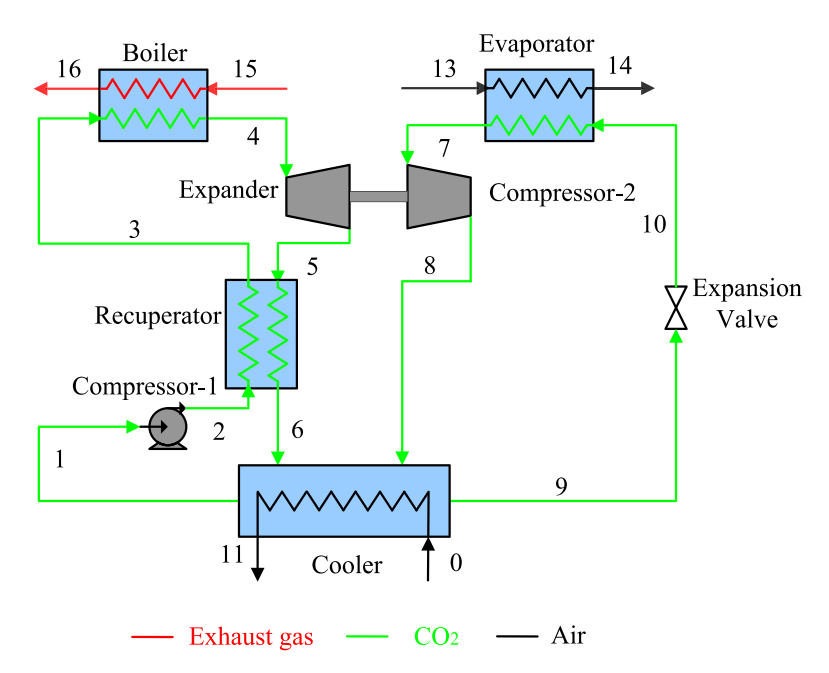


Fig. 10. Schematic diagram of the S-CO<sub>2</sub>/T-CO<sub>2</sub> combined cycle sharing a common cooler.

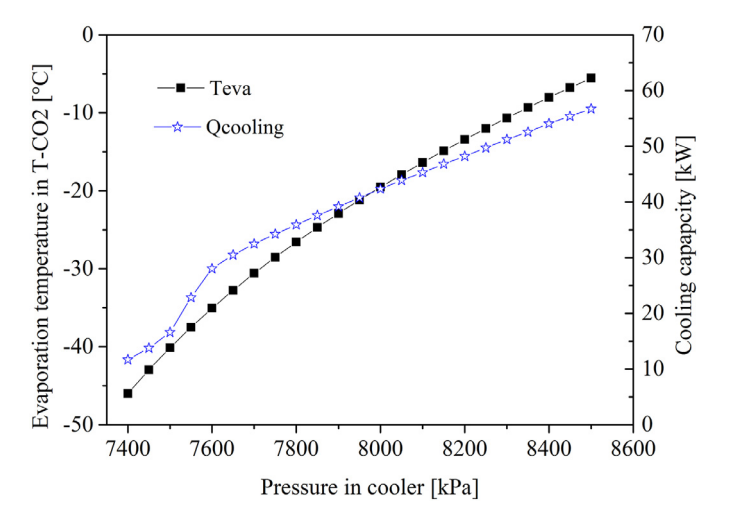


Fig. 12. Variation of evaporation temperature in T-CO<sub>2</sub> and cooling capacity with the pressure in cooler.

versibilities that exist in these components by design. Irreversibility of compressor and expander basically depend on their isentropic efficiency, so proper design of compressor and expander can reduce this irreversibility. To reduce the irreversibility of evaporator, cooler and boiler, they are to be designed in such a way that the temperature difference between the fluids can be maintained as small as possible.

### 5.2.2. Fixed evaporation pressure

In this part, the evaporation temperature in T-CO $_2$  cycle is fixed to be -15 °C, and the CO $_2$  temperature exiting the cooler and the maximum temperature in S-CO $_2$  is 32 °C and 380 °C, respectively. In that case, the high-side pressure in S-CO $_2$  (expander inlet pressure) varies linearly with the pressure in cooler.

Fig. 14 shows the variation of the powers and its thermal efficiency in the  $S-CO_2$  cycle with the increasing discharge pressure. It can be observed that both the power output of expander and the pump power show a similar variation trend, increasing first and then decreasing, finally become unchanged above 7700 kPa. As mentioned above, the thermophysical properties of  $CO_2$  changes

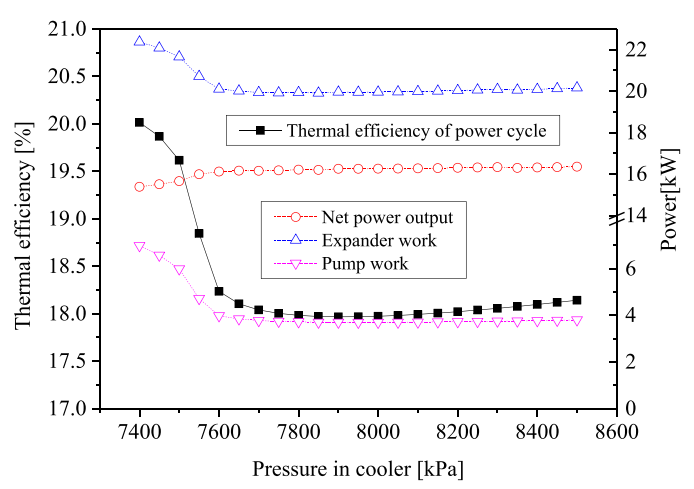


**Fig. 14.** Variation of thermal efficiency, expander power, pump work and the net power output of the S-CO<sub>2</sub> power cycle.

dramatically with temperature and pressure in the supercritical region. In this system, the  $CO_2$  temperature exiting cooler is set to be 32 °C. As mentioned above, when the discharge pressure is 7.45 Mpa, its corresponding pseudo-critical point appears at temperature 32 °C (305K) and an isobaric heat capacity presents a peak value, leading to peak value for  $h_1$  as well at this pseudo-critical point. As a result,  $h_2$  and  $h_3$  also reach peak values under this point. Subsequently, the enthalpy difference  $(h_4$ - $h_3)$  becomes smaller for a fixed high temperature  $T_4$  of 380 °C. For this reason, the mass flow rate increases to the maximum and the power generated in the expander reaches its maximum value. The same explanation can also apply to the case of the pump work. The maximum thermal efficiency of S- $CO_2$  is obtained at pseudo-critical point, which is 20%

Exergy destructions for the components in the proposed system are shown in Fig. 15. The exergy analysis results demonstrate the irreversibility of the recuperator, the expansion valve, evaporator and the cooler vary a lot when discharge pressure is operated close to the pseudo-critical point (ranging from 7400kPa to 7600 kPa). It can be attributed to the dramatic change of specific heat capacity near the pseudo-critical point. When the discharge pres-

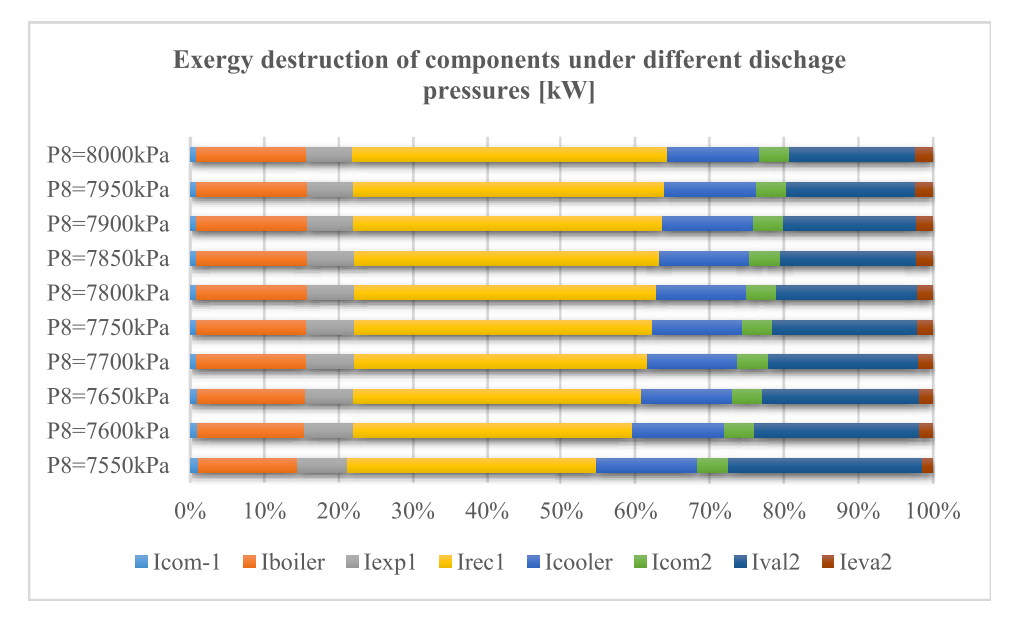
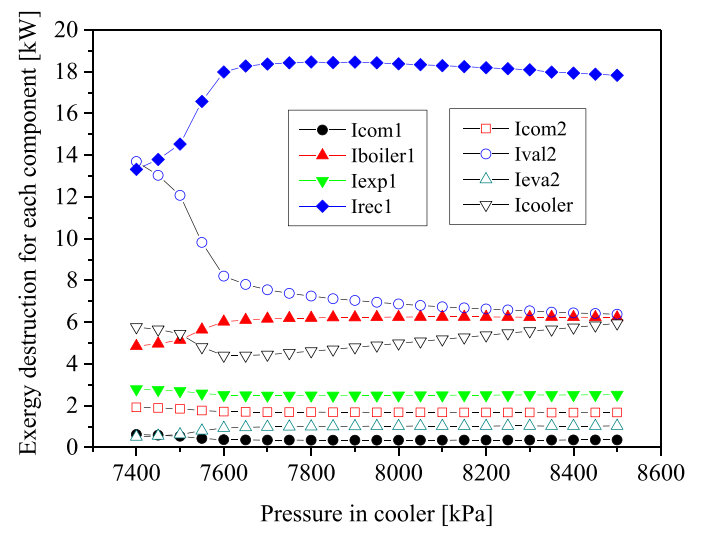


Fig. 13. Contribution of each component on the exergy destruction under different pressures in the cooler.

**Table 4** Comparison between two layouts under optimal condition (maximum cooling capacity), the ambient temperature  $T_0$ =25 °C and the evaporation temperature  $T_{eva}$ =-15 °C.

parameters	System with two separate coolers	System sharing a common cooler
Cooling capacity [kW]	59.47	46.86
Consumed power by compressor-1	9.63	3.75
COP	1.95	2.33
Net power output of S-CO2 [kW]	20.88	16.336
Thermal efficiency of S-CO2 [%]	24.26	18.06
Exergy efficiency [%]	12.52	10.64



**Fig. 15.** Exergy destruction of each component with the variation of condensation pressure.

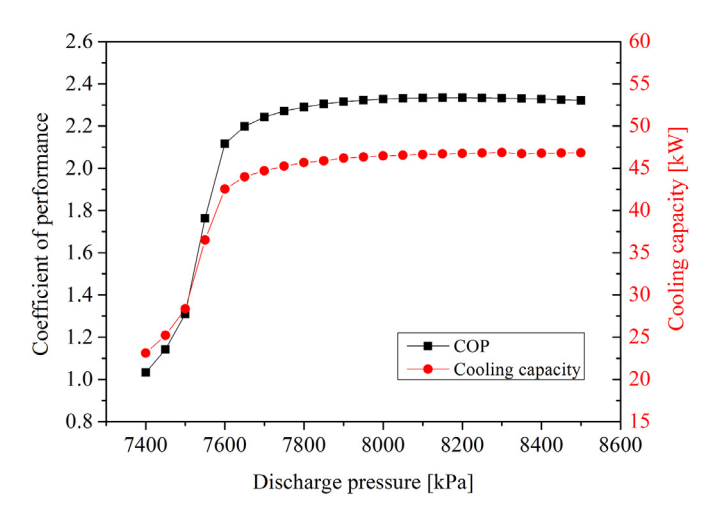


Fig. 16. Cooling coefficient of performance and cooling capacity in T-CO2.

sure keep increasing, the effect of discharge pressure on the irreversibility becomes minor.

Fig. 16 shows the variation of cooling coefficient performance and cooling capacity with the increasing discharge pressure in the T-CO<sub>2</sub>. The COP and cooling capacity show a similar variation trend, which increases first and then decreases slightly. The variation of the discharge pressure has minor effect on cooling capacity and COP when it is higher than 7600 kPa. In the T-CO<sub>2</sub> refrigeration cycle, as the discharge pressure increases, the power consumed by compressor increases. Furthermore, when the discharge pressure is higher than 7600 kPa, the cooling capacity is about 37.5

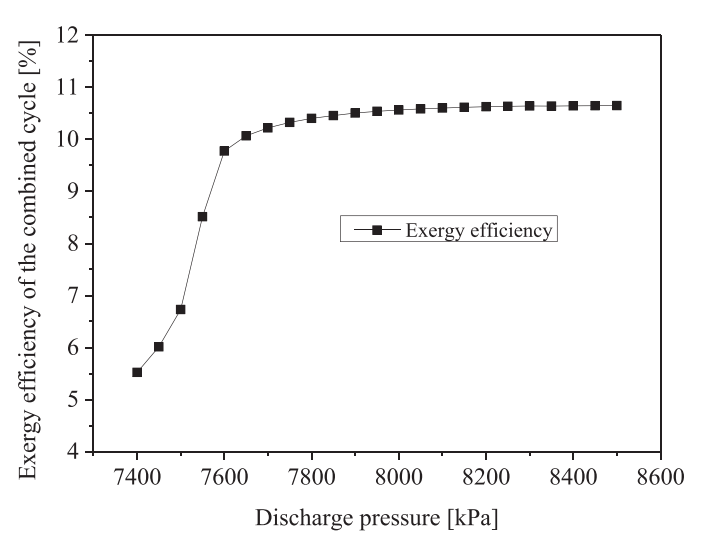


Fig. 17. Exergy efficiency of the combined cycle.

kW, which is comparable with that of the first layout that uses two separate coolers for S-CO<sub>2</sub> and T-CO<sub>2</sub> (shown in Fig. 6). It can be concluded that the S-CO<sub>2</sub>/T-CO<sub>2</sub> combined cycle sharing a common cooler has greater potential in practical application for its compactness

The variation of exergy efficiency of the combined cycle shown in Fig. 17 is similar to that of the cooling capacity shown in Fig. 16 The exergy efficiency is raised dramatically with the discharge pressure ranging from 7400 kPa to 7600 kPa. When the discharge pressure is higher above 7600 kPa, the effect of the discharge pressure on the exergy efficiency is minor and it is around of the cooling to the cooling that the cooling capacity shown in Fig. 16 The exergy efficiency is raised dramatically with the discharge pressure ranging from 7400 kPa to 7600 kPa. When the discharge pressure is higher above 7600 kPa, the effect of the discharge pressure on the exergy efficiency is minor and it is around the cooling that the cooling t

In order to compare the performance, the evaporation temperature in these two layouts is set to be the same. In that case, it can be taken as the optimal condition when the cooling capacity reaches the peak value. The results shown in Table 4 are operated when the maximum cooling capacity is obtained. From the comparison in table 4, the S-CO<sub>2</sub>/T-CO<sub>2</sub> combined system with two separate coolers shows a cooling capacity 8% higher than with that sharing a common cooler. However, the system with only one cooler has advantage in the size and weight for the practical application. Technical-economic evaluation is required in the further investigation before the system designs.

### 6. Conclusions

This paper proposes a refrigeration system that essentially integrates a S-CO $_2$  power cycle and a T-CO $_2$  refrigeration combined cycle by waste heat recovery of engine. The heat energy of the exhaust gas is recovered by a S-CO $_2$  power cycle, in which the produced power is use to power two compressors. Cooling is supplied to the cabinet by T-CO $_2$  refrigeration cycle. Furthermore, two dif-

ferent layout are analysed and compared. The analyses led to the following conclusions:

- The recuperator and the expansion valve contribute the most significant part of the total exergy destruction in S-CO<sub>2</sub> and T-CO<sub>2</sub>, respectively.
- (2) Compared with the system with two separated coolers, the system sharing a common cooler has comparable cooling capacity with the same refrigeration temperature but more compact.
- (3) With respect to the layout sharing a common cooler, the performance is improved when the discharge pressure increases from 7400 to 7600 kPa but the improvement becomes minor when the discharge pressure is further increased.
- (4) The proposed S-CO<sub>2</sub>/T-CO<sub>2</sub> combined cycle is feasible to provide sufficient cooling capacity for the refrigerated truck cabinet with more than 105 m<sup>2</sup> surface area.

### **Declaration of interests**

The authors declare that they have no known competing financial interests or personal relationships that could have appeared to influence the work reported in this paper.

### Acknowledgment

This research is funded by EPSRC (EP/N020472/1, EP/N005228/1, EP/R003122/1, and EP/P028829/1) in the United Kingdom.

### References

- Ahn, Y., Bae, S.J., Kim, M., Cho, S.K., Baik, S., Lee, J.I., Cha, J.E., 2015. Review of supercritical CO<sub>2</sub> power cycle technology and current status of research and development. Nucl. Eng. Technol. 47 (6), 647–661.
- Angelino, G., 1968. Carbon dioxide condensation cycles for power production. Journal of Engineering for Power 90 (3), 287–295.
- Aphornratana, S., Sriveerakul, T., 2010. Analysis of a combined Rankine-vapor-compression refrigeration cycle. Energy Convers. Manag. 51 (12), 2557–2564.
- Baheta, A.T., Hassan, S., Reduan, A.R.B., et al., 2015. Performance investigation of transcritical carbon dioxide refrigeration cycle. Procedia Cirp 26, 482–485.
- Chinen, T., Kato, H., Ichihara, M., Mizuno, H., 2014. Development of Rotary Compressor for High-efficiency CO<sub>2</sub> Heat-pump Hot-Water Supply System. In: International compressor engineering conference. Purdue.
- Combs, O.V., 1977. An investigation of the supercritical CO2 cycle (Feher cycle) for shipboard application (Doctoral dissertation. Massachusetts Institute of Technology).
- Dolz, V., Novella, R., García, A., Sánchez, J., 2012. HD Diesel engine equipped with a bottoming Rankine cycle as a waste heat recovery system. Part 1: Study and analysis of the waste heat energy. Appl. Therm. Eng. 36, 269–278.
- Dreiman, N., Bunch, R., Hwang, Y.H., Radermacher, R., 2004. Two-stage rolling piston carbon dioxide compressor. In: International compressor engineering conference. Purdue.
- Feher, E., 1968. The supercritical thermodynamic power cycle. Energy Convers. Manag 8, 85–90.
- Fernández-Seara, J., Vales, A., Vázquez, M., 1998. Heat recovery system to power an onboard NH<sub>3</sub>-H<sub>2</sub>O absorption refrigeration plant in trawler chiller fishing vessels. Appl. Therm. Eng. 18 (12), 1189–1205.
- Gao, P., Wang, L.W., Wang, R.Z., et al., 2016. Experimental investigation of a MnCl2/CaCl2-NH3 two-stage solid sorption freezing system for a refrigerated truck. Energy 103, 16–26.
- Gao, P., Wang, L.W., Wang, R.Z., Zhang, X.F., Li, D.P., Liang, Z.W., Cai, A.F., 2016. Experimental investigation of a MnCl2/CaCl2-NH3 two-stage solid sorption freezing system for a refrigerated truck. Energy 103, 16–26.
- Gao, J., Wang, L.W., Gao, P., et al., 2019. Performance investigation of a freezing system with novel multi-salt sorbent for refrigerated truck. International Journal of Refrigeration 98, 129–138.
- Hinderink, A.P., Van der Kooi, H.J., De Swaan Arons, J., 1999. On the efficiency and sustainability of the process industry. Green Chem 1, G176–G180. doi:10.1039/ A909915H, http://dx. doi.org/.
- International Institute of Refrigeration. Guide to refrigerated transport; 1995.
- Kim, S.C., Won, J.P., Kim, M.S., 2009. Effects of operating parameters on the performance of a CO2 air conditioning system for vehicles. Appl. Therm. Eng. 29 (11–12), 2408–2416.

- Li, H., Bu, X., Wang, L., Long, Z., Lian, Y., 2013. Hydrocarbon working fluids for a Rankine cycle powered vapor compression refrigeration system using low-grade thermal energy. Energy Build 65, 167–172.
- Liang, Y., Shu, G., Tian, H., Liang, X., Wei, H., Liu, L., 2013. Analysis of an electricity-cooling cogeneration system based on RC-ARS combined cycle aboard ship. Energy Convers. Manag. 76, 1053–1060.
- Liang, Y., Shu, G., Tian, H., Wei, H., Liang, X., Liu, L., Wang, X., 2014. Theoretical analysis of a novel electricity-cooling cogeneration system (ECCS) based on cascade use of waste heat of marine engine. Energy Convers. Manag. 85, 888–894.
- Liang, Y., Shu, G., Tian, H., Sun, Z., 2018. Investigation of a cascade waste heat recovery system based on coupling of steam Rankine cycle and NH3-H2O absorption refrigeration cycle. Energy Convers. Manag. 166, 697–703.
- Liang, Y., Al-Tameemi, M., Yu, Z., 2018. Investigation of a gas-fuelled water heater based on combined power and heat pump cycles. Appl. Energy 212, 1476– 1488.
- Liang, Y., Bian, X., Qian, W., Pan, M., Ban, Z., Yu, Z., 2019. Theoretical analysis of a regenerative supercritical carbon dioxide Brayton cycle/organic Rankine cycle dual loop for waste heat recovery of a diesel/natural gas dual-fuel engine. Energy Convers. Manag. 197, 111 845.
- Liu, Y., Leong, K.C., 2005. The effect of operating conditions on the performance of zeolite/water adsorption cooling systems. Applied Thermal Engineering 25, 1403–1418.
- Lorentzen, G., Pettersen, J., 1993. A new, efficient and environmentally benign system for car air-conditioning. Int. J. Refrig. 16 (1), 4–12.
- Ma, Y., Liu, Z., Tian, H., 2013. A review of transcritical carbon dioxide heat pump and refrigeration cycles. Energy 55, 156–172.
- Manente, G., Lazzaretto, A., 2014. Innovative biomass to power conversion systems based on cascaded supercritical CO2 Brayton cycles. Biomass And Bioenergy. 69, 155–168.
- Manzela, A.A., Hanriot, S.M., Cabezas-Gómez, L., Sodré, J.R., 2010. Using engine exhaust gas as energy source for an absorption refrigeration system. Appl. Energy. 87 (4), 1141–1148.
- Ohkawa, T., Kumakura, E., Higashi, H., Sakitani, K., Higuchi, M., Taniwa, H., Ozawa, H., 2002. Development of Hermetic Swing Compressors For CO2 Refrigerants. In: The proceeding of the 16th international compressor engineering conference. Purdue.
- Persichilli, M., Held, T., Hostler, S., Zdankiewicz, E., Klapp, D., 2011. Transforming waste heat to power through development of a CO<sub>2</sub>-based-power cycle. Electric Power Expo 10–12.
- Persichilli, M., Kacludis, A., Zdankiewicz, E. and Held, T., 2012. Supercritical CO2 power cycle developments and commercialization: why sCO2 can displace steam ste. Power-Gen India & Central Asia.
- Pettersen, J., 1994. An efficient new automobile air-conditioning system based on CO<sub>2</sub> vapor compression (No. CONF-9,406,105-). American Society of Heating, Refrigerating and Air-Conditioning Engineers, Inc., Atlanta, GAUnited States.
- Prigmore, D., Barber, R., 1975. Cooling with the sun's heat Design considerations and test data for a Rankine Cycle prototype. Sol. Energy. 17 (3), 185–192.
- Protocol, M., 1987. Montreal protocol on substances that deplete the ozone layer, 26. Government Printing Office, Washington, DC: US, pp. 128–136.
- Ruthven, D.M., 1984. Principles of adsorption and adsorption processes. Wiley, New York.
- Saleh, B., 2016. Parametric and working fluid analysis of a combined organic Rankine-vapor compression refrigeration system activated by low-grade thermal energy. J. Adv. Res. 7 (5), 651–660.
- Sarkar, J., 2015. Review and future trends of supercritical CO2 Rankine cycle for lowgrade heat conversion. Renew. Sustain. Energy Rev. 48, 434–451.
- Sharma, O.P., Kaushik, S.C., Manjunath, K., 2017. Thermodynamic analysis and optimization of a supercritical CO2 regenerative recompression Brayton cycle coupled with a marine gas turbine for shipboard waste heat recovery. Thermal Science and Engineering Progress 3, 62–74.
- Shu, G., Liang, Y., Wei, H., Tian, H., Zhao, J., Liu, L., 2013. A review of waste heat recovery on two-stroke IC engine aboard ships. Renew. Sustain. Energy Rev. 19, 385–401.
- Song, J., Li, X.S., Ren, X.D., Gu, C.W., 2018. Performance analysis and parametric optimization of supercritical carbon dioxide (S-CO<sub>2</sub>) cycle with bottoming Organic Rankine Cycle (ORC). Energy 143, 406–416.
- Stosic, N., Smith, I.K., Kovacevic, A., 2002. A twin screw combined compressor and expander for CO<sub>2</sub> refrigeration systems. In: International compressor engineering conference., Purdue, p. 2002.
- Sun, J., Li, W., Cui, B., 2019. Energy and exergy analyses of R513a as a R134a drop-in replacement in a vapor compression refrigeration system. International Journal of Refrigeration 112, 348–356.
- Tao, Y.B., He, Y.L., Tao, W.Q., 2010. Exergetic analysis of transcritical CO2 residential air-conditioning system based on experimental data. Appl. Energy. 87 (10), 3065–3072
- Tassou, S.A., De-Lille, G., Lewis, J., 2012. Food Trasport Refrigeration. center for Energy and Built Environment Research. Brunel University, UK.
- Tiwari, H., Parishwad, G.V., 2012. Adsorption refrigeration system for cabin cooling of trucks. International journal of emerging technology and advanced engineering 2 (10), 337–342.
- Wang, H., Peterson, R., Harada, K., Miller, E., Ingram-Goble, R., Fisher, L., Yih, J., Ward, C., 2011. Performance of a combined organic Rankine cycle and vapor compression cycle for heat activated cooling. Energy 36 (1), 447–458.
- Wang, H., Peterson, R., Herron, T., 2011. Design study of configurations on system COP for a combined ORC (organic Rankine cycle) and VCC (vapor compression cycle). Energy 36 (8), 4809–4820.

- Wang, K., He, Y.L., Zhu, H.H., 2017. Integration between supercritical CO2 Brayton cycles and molten salt solar power towers: A review and a comprehensive comparison of different cycle layouts. Appl. Energy. 195, 819–836.
  Wang, R.Z., Oliveira, R.G., 2006. Adsorption refrigeration-an efficient way to make good use of waste heat and solar energy. Progress in Energy and Combustion Science 32 (4), 424–458.
- Zheng, J., Wang, J., Zhao, Z., Wang, D., Huang, Z., 2019. Effect of equivalence ratio on combustion and emissions of a dual-fuel natural gas engine ignited with diesel.
- Appl. Therm. Eng. 146, 738–751.

  Zhu, F.Q., Jiang, L., Wang, L.W., et al., 2016. Experimental investigation on a MnCl2CaCl2NH3 resorption system for heat and refrigeration cogeneration. Applied energy 181, 29-37.